Proton-Proton Scattering at Low Energies

M. D. Barker, P. C. Colby, and W. Haeberli
University of Wisconsin, Madison, Wisconsin 53706

and

P. Signell
Michigan State University, East Lansing, Michigan 48824
(Received 16 February 1982)

The analyzing power in proton-proton scattering has been measured at bombarding energies of 5.05 and 9.85 MeV to an accuracy of $\pm 5\times 10^{-5}$. The measurements were combined with existing cross-section data to obtain model-independent S- and P-wave phase shifts at these energies. In addition, the first experimental determination of the P-wave scattering lengths and effective ranges is reported. These are compared to model values and their use in obtaining improved S-wave parameters is suggested.

PACS numbers: 25.40.Cm, 21.30.+y, 24.70.+s, 25.10.+s

We report new proton-proton analyzing-power measurements at laboratory energies of 5 and 10 MeV. These data, along with existing precision cross-section measurements,[1-3] enable us to determine the first experimental values of the proton-proton P-wave effective-range parameters. The resulting effective-range parameters are of sufficient accuracy to establish significant constraints upon interaction models with adjustable parameters, such as the Paris potential.[4] Furthermore they provide, for the first time, values of the P-wave interaction needed for analyses of the large quantity of high-accuracy cross-section data that has been measured at energies below 10 MeV. Of particular interest in this regard are the precision angular distributions at various energies up to 1 MeV,[5] especially the very accurate cross-section measurements in the region of the Coulomb-nuclear interference minimum at 0.38 MeV.

Analyzing-power measurements were made at eleven scattering angles at 5.05 ± 0.03 MeV and fifteen angles at 9.85 ± 0.03 MeV to an accuracy of $\pm 5\times 10^{-5}$. This is a factor-of-6 improvement in precision over the previous measurements at 6.141 MeV,[6] and a factor-of-4 improvement over the measurements at 10.0 MeV.[7] The analyzing power was determined by bombarding a target of gaseous hydrogen with polarized protons and measuring the left-right asymmetry of the scattered protons with detectors placed symmetrically about the beam direction. A tandem electrostatic accelerator equipped with a colliding-beams ion source[8] produced the spin-polarized beam. The spin state was reversed every 0.25 sec by alternately energizing a weak-field and a strong-field rf transition unit. A spin precessor[9] (prior to injection) oriented the spin axis perpendicular to the reaction plane. The beam polarization for each spin state (typically 0.84 to 0.88) was continuously monitored by observing the left-right asymmetry of protons scattered from ^{4}He in a polarimeter mounted directly behind the main scattering chamber.

The incident beam was defined by a 1.0×2.0-mm^2 slit located 0.36 m from the center of the target. A second slit, 2.6 m from the target, defined the direction of the beam to ± 1.1 mrad. The entire scattering chamber was filled with 300 Torr of hydrogen gas (99.999% purity) with the beam entering through a 0.5-μm Ni foil located 0.37 m from target center. Two antiscattering slits were located after the beam-defining slit to shield the front slit of the detector slit system from protons scattered by the foil and by slit edges. The beam-defining and antiscattering slits were such that each antiscattering slit was in the shadow formed by the previous slit.

Both Si surface barrier detectors and CsI(Th) scintillators were used to detect scattered protons. At each scattering angle, the detector and detector slit geometry were chosen such that protons elastically scattered from contaminants (other than deuterium) were resolved from those scattered from protons. The detector apertures were placed 20 cm from the center of the target, except at $\theta_{\rm lab}=7.5°$ and 10° where the apertures were 40 cm from target center. The extreme angular acceptance of the detector slit systems ranged from $\pm 2.0°$ at $\theta_{\rm lab}=45°$ to $\pm 0.3°$ at $\theta_{\rm lab}=7.5°$. The actual scattering angles defined by the detector slit systems were determined with an alignment telescope to an accuracy of $\pm 0.06°$.

To obtain an accurate measurement of the ana-

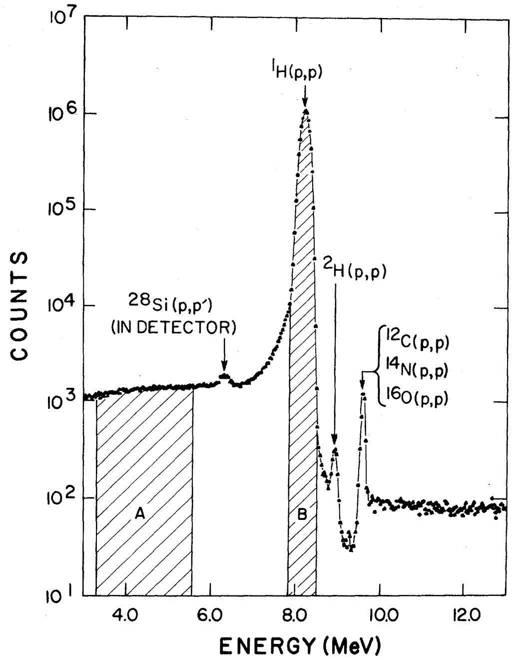

FIG. 1. Pulse height spectrum at $\theta_{lab} = 22.5°$ for a proton bombarding energy of 9.85 MeV. The low-energy tail of the p-p peak is due to incomplete charge collection in the solid-state detector. The background above 10 MeV is due to pileup. Also evident are the elastic scattering peaks from deuterium and other contaminants on the high-energy side of the p-p peak.

TABLE I. p-p analyzing powers.

E_{lab} = 5.05 MeV		E_{lab} = 9.85 MeV	
$\theta_{c.m.}$[a] (deg)	$A \times 10^4$	$\theta_{c.m.}$[a] (deg)	$A \times 10^4$
19.95	-5.21 ± 0.51	15.36	-15.44 ± 0.56
24.59	-6.47 ± 0.55	20.47	-20.79 ± 0.38
30.60	-5.82 ± 0.47	25.63	-19.14 ± 0.44
40.35	-3.26 ± 0.40	30.64	-14.54 ± 0.55
44.47	-3.10 ± 0.51	35.57	-11.75 ± 0.37
50.54	-2.16 ± 0.32	40.52	-8.46 ± 0.26
60.23	-1.79 ± 0.40	45.53	-5.40 ± 0.52
64.31	-1.28 ± 0.52	50.54	-4.36 ± 0.58
70.43	-0.35 ± 0.37	55.55	-3.30 ± 0.45
80.32	-0.26 ± 0.58	60.43	-2.48 ± 0.30
90.32	$+0.40 \pm 0.49$	65.38	-2.33 ± 0.53
		70.56	-0.74 ± 0.37
		75.38	-0.70 ± 0.41
		80.39	-0.73 ± 0.52
		90.39	-0.37 ± 0.45

[a] All c.m. angles are calculated using the relativistic transformation.

lyzing power, one must ascertain that no significant background or contaminants lie under the p-p peak of the detector pulse-height spectra. The flat background on the low-energy side of the p-p peak (see Fig. 1) is characteristic of slit-edge scattering. The assumption that this low-energy background arises from small-angle scattering by slit edges is supported by the fact that its analyzing power (measured to $\pm 7 \times 10^{-4}$) agrees with the p-p analyzing power at each angle. A typical region used to make this measurement is labeled A in Fig. 1. The ratio of the number of events in the p-p peak (labeled B) to those in the background under the peak is greater than 250. This implies an upper bound of $\pm 3 \times 10^{-6}$ to the error caused by slit-edge scattering. Elastic scattering from contaminants is clearly separated from p-p scattering (Fig. 1). No evidence for inelastic scattering from contaminant gases was seen in the pulse-height spectra. Furthermore, an estimate of the contribution of inelastic scattering based on the likely elemental composition of the contaminant gases and known inelastic and elastic cross sections indicates that this

TABLE II. Comparison of the low-L nuclear bar "electric" phase parameters (in degrees) at 5.05 and 9.85 MeV obtained from our "single-energy" analyses to those calculated from the Paris potential (Ref. 4).

	$^1S_0$	$^3P_0$	$^3P_1$	$^3P_2$
		E_{lab} = 5.05 MeV		
Our analysis[a]	54.60 ± 0.11	1.63 ± 0.09	-0.843 ± 0.028	0.254 ± 0.019
Paris potential	54.92	1.95	-1.090	0.268
		E_{lab} = 9.85 MeV		
Our analysis[a]	55.24 ± 0.15	3.22 ± 0.07	-1.916 ± 0.025	0.631 ± 0.019
Paris potential	55.19	3.82	-2.087	0.634

[a] The higher partial waves are consistent with the Paris potential (Ref. 4).

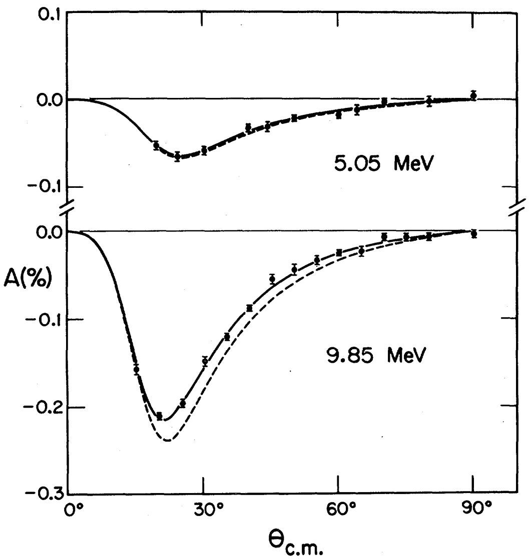

FIG. 2. Proton-proton analyzing power at 5.05 and 9.85 MeV plotted as a function of c.m. scattering angle. The solid curves through the data points are obtained from our phase-shift analyses. The dashed curves are the analyzing powers predicted from the Paris potential.

contribution is less than $\pm 10^{-6}$. At those angles where the p-d contaminants were not resolved from the p-p peak, the resultant analyzing powers were corrected by use of the known abundance, cross-section,[10] and analyzing powers[11] of p-d scattering. This correction was less than 4×10^{-6}.

There is also an uncertainty in the analyzing power associated with the uncertainty in the angular position of the detectors. This uncertainty, translated into an error in the analyzing power, is significant ($\pm 1.5\times10^{-5}$) only for $\theta_{\rm lab} = 7.5°$ at 9.85 MeV. The dead time of the detection electronics was measured and resulted in a correction which is 2% of the measured analyzing power. The corrected analyzing powers are presented in Table I. The uncertainties were obtained by adding the various errors discussed above in quadrature with the statistical uncertainty. The statistical error of the beam polarization measurement is included, but not a 1% scale error which arises from the uncertainty in the analyzing power of the polarimeter reaction.[12]

The data were analyzed in two ways. First, values of the S- and P-wave phase shifts were found in the neighborhood of 5 and 10 MeV using "single-energy" phase-shift analyses. Second, the data sets at 5 and 10 MeV were combined with previously obtained $^3P_1$ and $^3P_2$ phase shifts at 25 MeV,[13] to determine the S- and P-wave scattering lengths and effective ranges. The analysis methods used were described by Sher, Signell, and Heller.[14]

Phase shifts at 5 and 10 MeV were obtained from the measurements reported here and the cross-section data of Imai, Nisimura, and Tamura[1] at 4.978 MeV, Johnston and Young[2] at 9.69 MeV, and Hegland *et al.*[3] at 9.918 MeV. Other nearby data were omitted on the grounds that they were inconsistent with two or more other data sets or were too imprecise to have a significant effect on the analysis. The resulting phase shifts are shown in Table II where they are compared to values we calculated from the widely used Paris potential.[4] The analyzing powers calculated from the phase shifts of Table II are shown in Fig. 2, along with the measurements reported here, and the predictions of the Paris potential.

The effective-range parameters were obtained by combining the 5- and 10-MeV data sets with the $^3P_1$ and $^3P_2$ phase parameters at 25 MeV.[13] The present analyses corroborated Naisse's assertion[15] that the effective-range function for the $^3P_0$ state has too much curvature to be adequately represented above 10 MeV by only two terms of the effective-range series. However, within the present experimental uncertainties, we find no evidence of curvature in the $^3P_1$ function and the subtracted $^3P_2$ function (see Ref. 14) up to 25 MeV. The resulting scattering lengths and effective

TABLE III. Scattering lengths (in femtometers) and effective ranges (in inverse femtometers) for each of three P states.

	a_{1J}			r_{1J}		
	$^3P_0$	$^3P_1$	$^3P_2$	$^3P_0$	$^3P_1$	$^3P_2$
Our analysis	-4.82 ± 1.11	1.78 ± 0.10	-0.317 ± 0.023	7.14 ± 0.93	-7.85 ± 0.52	7.5 ± 2.9
Nagels *et al.*[a]	-3.00	1.82	-0.28	3.44	-7.49	4.5
Nagels *et al.*[b]	-2.84	1.99	-0.29	2.46	-7.56	4.4
Paris potential	-3.42	2.05	-0.30	4.00	-7.69	5.7

[a]Ref. 17. [b]Ref. 16.

ranges are shown in Table III along with values from one-boson exchange potentials[16,17] and the Paris potential.[4] All three of these potentials contain adjustable parameters, which would now seem to require some additional adjusting.

The effective-range parameters we report here imply that the "central" combination of P waves follows the "*BA*" curve in Fig. 12 of Sher, Signell, and Heller[14] at all energies. This central combination is the only P-wave component needed to analyze the extremely accurate and extensive cross-section measurements that have been made below 1 MeV. Because the central P-wave combination is now sufficiently well known, a reanalysis of low-energy cross-section data will yield substantially improved values for the S-wave effective range parameters. It will be very interesting to compare these improved S-wave parameters to values from various models, just as was done here for the P-wave values.

We would like to thank Michael Brandl and Eugene Kales for their assistance with the analyses, and J. Ulbricht for help in the early stages of the experiment.

This work was supported in part by the U. S. Department of Energy.

[1]K. Imai, K. Nisimura, and N. Tamura, Nucl. Phys. A246, 76 (1975).

[2]L. H. Johnston and D. E. Young, Phys. Rev. 116, 989 (1959).

[3]P. M. Hegland, R. E. Brown, J. S. Lilley, and J. A. Koepke, Phys. Rev. Lett. 39, 9 (1977); P. M. Hegland, Ph.D. thesis, University of Minnesota, 1976 (unpublished).

[4]M. Lacombe *et al.*, Phys. Rev. C 21, 861 (1980).

[5]C. Thomann, J. E. Benn, and S. Munch, in *Nucleon-Nucleon Interactions—1977*, edited by H. Fearing, D. Measday, and A. Strathdee, A.I.P. Conference Proceedings No. 41 (American Institute of Physics, New York, 1978), p. 86.

[6]G. Bittner and W. Kretshmer, Phys. Rev. Lett. 43, 330 (1979).

[7]J. D. Hutton, W. Haeberli, L. D. Knutson, and P. Signell, Phys. Rev. Lett. 35, 429 (1975).

[8]W. Haeberli *et al.*, to be published.

[9]The spin precessor is a crossed-field analyzer purchased from ANAC Inc., Model No. 2171.

[10]D. C. Kocher and T. B. Clegg, Nucl. Phys. A132, 455 (1969).

[11]T. B. Clegg and W. Haeberli, Nucl. Phys. A95, 608 (1967).

[12]P. Schwandt, T. B. Clegg, and W. Haeberli, Nucl. Phys. A163, 432 (1971).

[13]G. E. Bohannon, T. Burt, and P. Signell, Phys. Rev. C 13, 1816 (1976).

[14]M. S. Sher, P. Signell, and L. Heller, Ann. Phys. (N.Y.) 58, 1 (1970).

[15]J. P. Naisse, Nucl. Phys. A278, 506 (1977).

[16]M. M. Nagels, T. A. Rijken, and J. J. de Swart, in *Few Body Systems and Nuclear Forces*, edited by H. Zingl, M. Haftel, and H. Zankel (Springer-Verlag, Berlin, 1978), Vol. I, 17.

[17]M. M. Nagels, T. A. Rijken, and J. J. de Swart, in *Proceedings of the International Conference on Few Body Problems in Nuclear and Particle Physics, Laval University, Quebec City, Canada, 1974*, edited by R. J. Slobodrian, B. Cujec, and K. Ramavatram (Les Presses de l'Université Laval, Quebec City, Canada, 1975), p. 27.